Use of the Doppler spectral with to improve the estimation of the convective boundary layer height from UHF wind Profiler observations

Bok-Haeng Heo, Sandra Jacoby-Koaly, Kyung-Eak Kim, Bernard Campistron, Bruno Bénech, Eun-Sil Jung

NOTES AND CORRESPONDENCE

Use of the Doppler Spectral Width to Improve the Estimation of the Convective Boundary Layer Height from UHF Wind Profiler Observations

BOK-HAENG HEO

Department of Astronomy and Atmospheric Sciences, Kyungpook National University, Daegu, South Korea

SANDRA JACOBY-KOALY

Laboratoire d'Aérologie (CNRS), Observatoire Midi-Pyrénées, Université Paul Sabatier, Toulouse, France

KYUNG-EAK KIM

Department of Astronomy and Atmospheric Sciences, Kyungpook National University, Daegu, South Korea

BERNARD CAMPISTRON AND BRUNO BENECH

Laboratoire d'Aérologie (CNRS), Observatoire Midi-Pyrénées, Université Paul Sabatier, Toulouse, France

EUN-SIL JUNG

Department of Astronomy and Atmospheric Sciences, Kyungpook National University, Daegu, South Korea

25 September 2000 and 2 August 2002

ABSTRACT

Enhancement of the air refractive index structure parameter C_n^2 often occurs at the top of the convective boundary layer (CBL), where the absolute values of the vertical gradients of virtual potential temperature and mixing ratio have a peak. This well-known behavior of the C_n^2 profiles is often used to locate the height of the mixed layer Z_i from UHF wind profiler observations. In the present study, Z_i determination with the C_n^2-based technique was investigated for a case of clear-air CBL and a case of cloud-topped CBL. In certain circumstances, such as multifold C_n^2 peaks or poorly defined peaks, these techniques fail to correctly retrieve CBL height. In order to improve Z_i determination, a new method based on the conjoint use of C_n^2 and Doppler spectral width profiles is proposed and discussed.

1. Introduction

The height of the atmospheric boundary layer Z_i governs the vertical mixing of atmospheric pollutant and has been used as an important parameter in air pollution monitoring and boundary layer studies. It is also an important scaling length for the normalization of boundary layer parameters such as fluxes and variance including vertical gradients of wind, potential temperature, and moisture. This characteristic level is required as a basic input parameter in numerical weather and climate forecasting models of the boundary layers (Stull 1988; Beyrich and Weill 1993).

The daytime continental convective boundary layer (CBL) considered in the present study is generally capped by a temperature inversion layer that arises in the morning in response to solar heating and the subsequent vertical mixing. It defines the interface between a well-mixed layer and the free atmosphere and prevents the vertical exchange of pollutants toward the free atmosphere. This interfacial layer called the entrainment zone is characterized by a significant vertical gradient of virtual potential temperature and a minimum heat flux. According to Stull (1988), the CBL height is the top of mixed layer, often defined as the average base of the overlying stable layer, and responds to surface forcings with a timescale of about an hour or less. Different definitions of CBL height have been proposed based on

Corresponding author address: Dr. Kyung-Eak Kim, Department of Astronomy and Atmospheric Sciences, Kyungpook National University, Daegu, 702-701, South Korea.
E-mail: kimke@knu.ac.kr

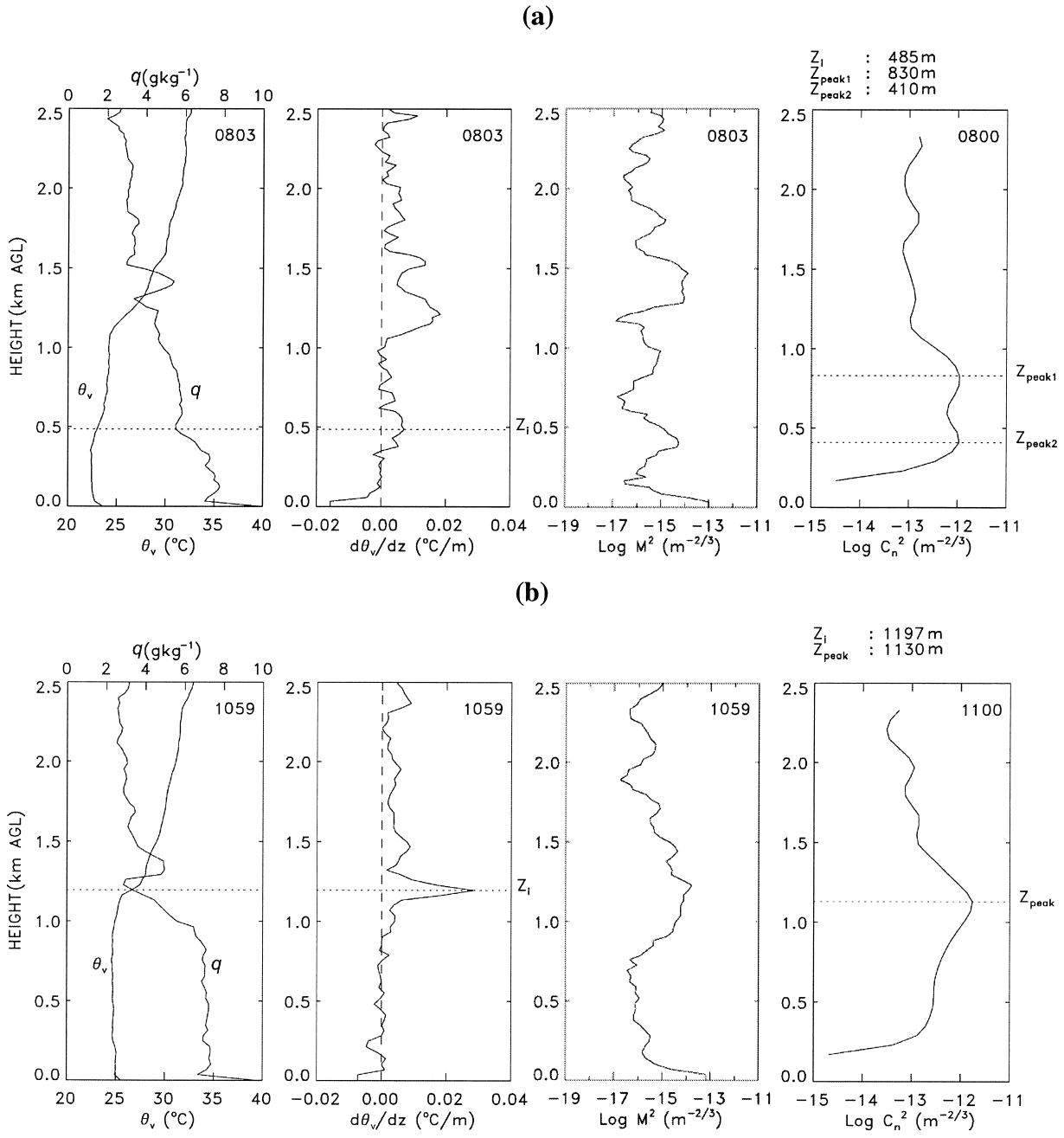

FIG. 1. Vertical profiles of the virtual potential temperature (θ_v), mixing ratio (q), virtual potential temperature gradient ($d\theta_v/dz$), and mean vertical gradient of potential refractivity (M^2) from rawinsonde observations at (a) 0803 and (b) 1059 LST, and C_n^2 profiles obtained from the UHF profiler observation on 19 Jun 1998 at Viabon. Parameter Z_i denotes the CBL height determined by the gradient method of Sullivan et al. (1998) from rawinsonde observations. Parameters Z_{peak1} (or Z_{peak}) and Z_{peak2} represent the primary and secondary peaks in C_n^2 profiles of the UHF profiler, respectively.

various physical quantities. Sullivan et al. (1998) defines Z_i as the height where the vertical gradient of potential temperature has its maximum value. This level corresponds to the middle of the inversion layer. It has also been defined as the height where the buoyancy flux reaches its most negative value (Deardorff et al. 1980; Wyngaard and LeMone 1980). In that case, the CBL height is defined as the base of the temperature inversion. During daytime, low and shallow stratus clouds can exist in or at the CBL top and often occupy a significant portion of the CBL. However, there is no consensus as to how to define CBL height in the presence of clouds. In that case, two characteristic levels are identified. The first one is the cloud base corresonding to

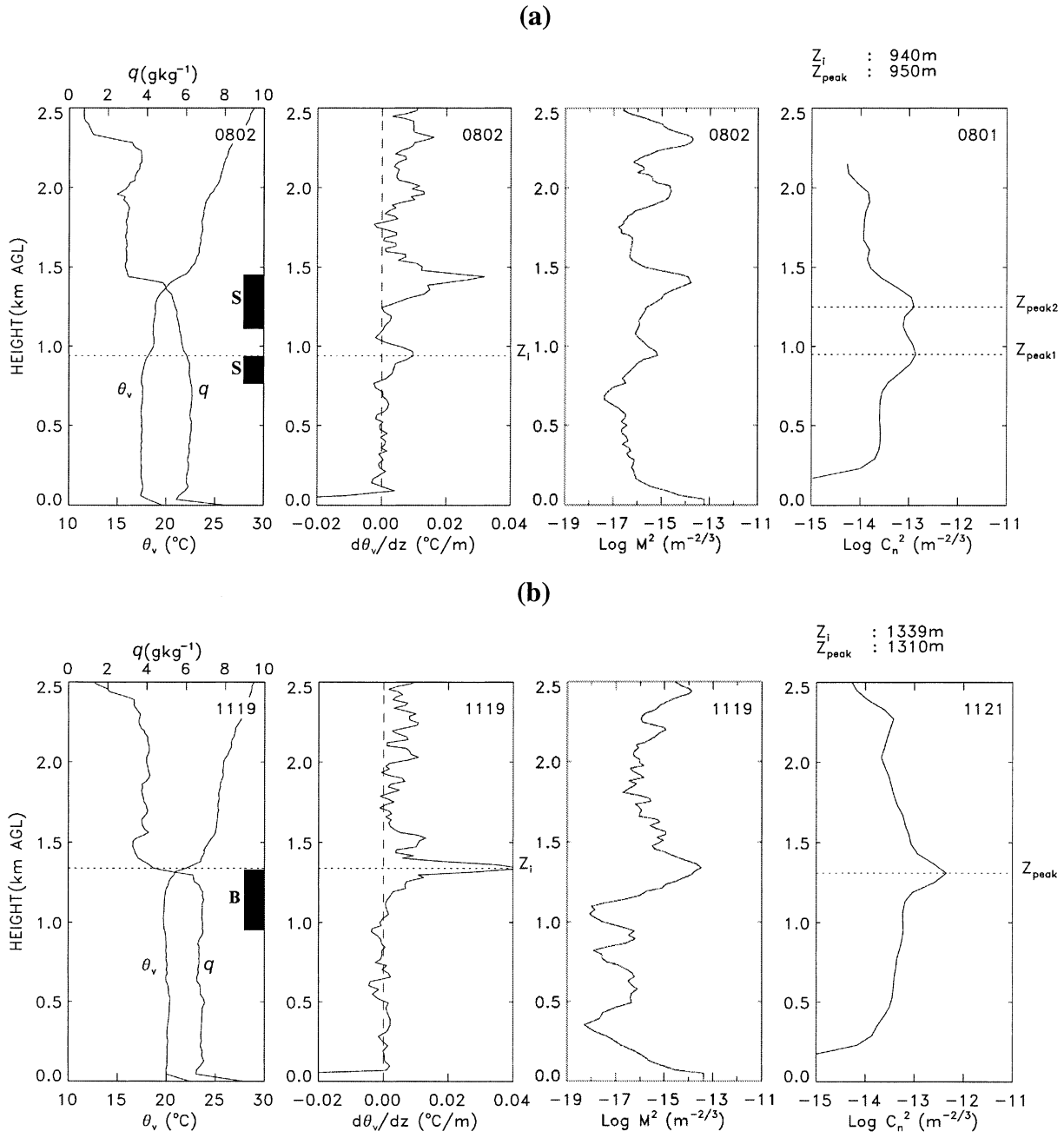

FIG. 2. As in Fig. 1, except for (a) 0802, (b) 1119, and (c) 1403 LST on 29 Jun 1998. Vertical solid bars with the B and S characters in the leftmost panel represent a cloud layer and broken and scattered clouds, respectively.

the height of dry mixing layer and the second one is the cloud top generally linked with the inversion layer. The difficulty in determining cloudy boundary layer height is due to the fact that a new turbulent source appears in the cloud layer linked with radiative and condensation/evaporation processes. This turbulent source can be strong at the cloud top and on the cloud edge when the cloud layer is fragmented. We will consider the case in which the cloud top corresponds to the Z_i level.

The entrainment in the interfacial layer can create a strong vertical gradient in the temperature and humidity profiles, which causes a maximum in the profile of the refractive index parameter C_n^2 resulting in an enhancement of sodar and ultrahigh frequency (UHF) profiler returns. A maximum value in backscattered intensity profiles can be also found in clouds because of the enhancement of reflectivity by strong turbulent mixing within the cloud and entrainment mixing near cloud boundaries (Angevine et al. 1994). Furthermore, the ra-

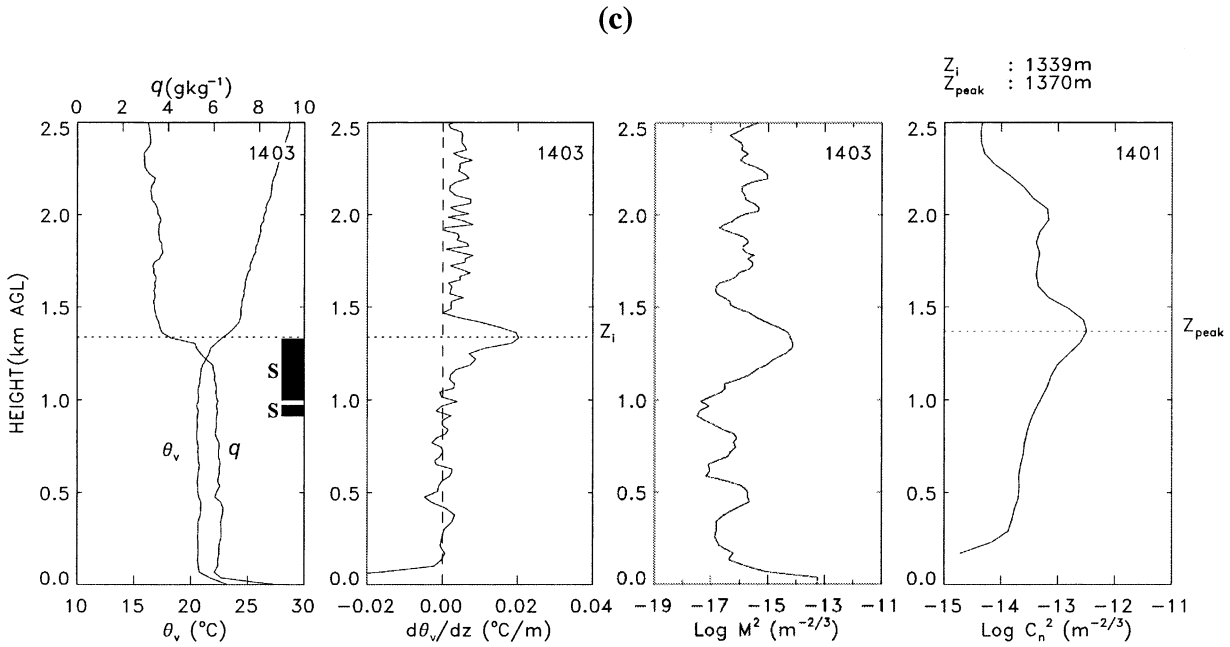

Fig. 2. (*Continued*)

dar backscattered intensity profiles can also present a maximum at the top of a residual layer, linked to the CBL developed on the previous day (Dye et al. 1995). Numerous studies based on numerical modeling and/or experimental data have shown that the vertical profiles of the refractive index structure parameter C_n^2 have a pronounced maximum near the base of the capping inversion layer or where the humidity gradient is large (Burk 1980; Wyngaard and LeMone 1980; Fairall 1991; Angevine et al. 1994; Muschinski et al. 1999). Benech et al. (1997) also showed with UHF observations that the C_n^2 peak occurred between the boundaries of temperature inversion layers and that the dissipation rate of turbulent kinetic energy significantly decreased near the base of the inversion. Grimsdell and Angevine (1998) showed that when a cloud layer of significant depth is present at the CBL top, the C_n^2 peak is poorly defined or displaced to the height of the cloud top or cloud edges.

Recently, different C_n^2-based techniques used to determine CBL height from the UHF profiler have been investigated. White (1993) estimated CBL height using

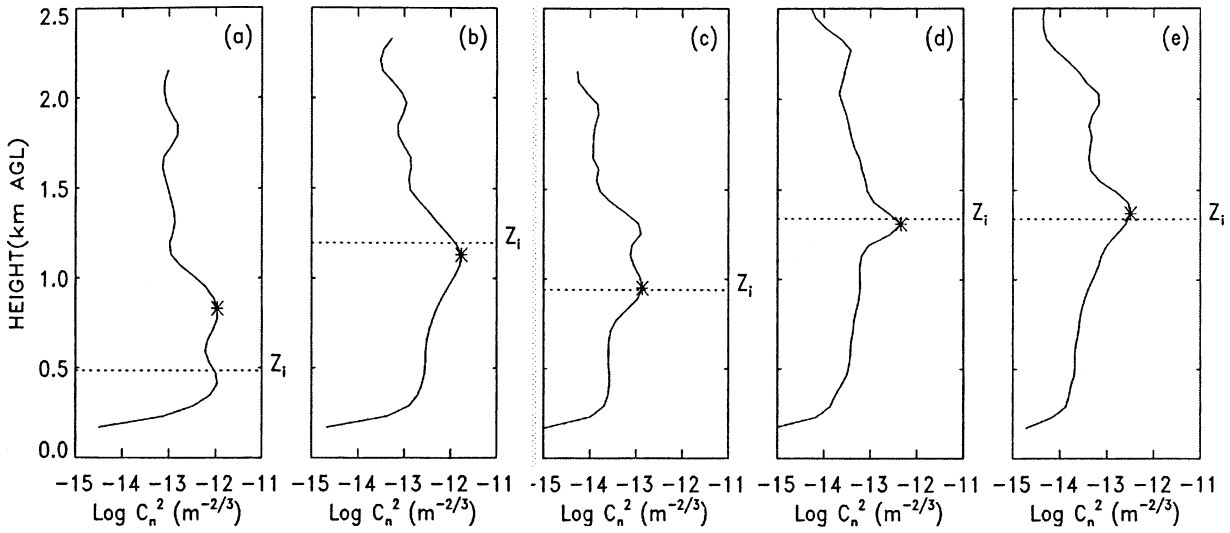

FIG. 3. Vertical profiles of the UHF backscatter intensity and CBL heights (asterisks) estimated by the maximum backscatter intensity method at (a) 0800 and (b) 1100 LST on 19 Jun, and (c) 0801, (d) 1121, and (e) 1401 LST on 29 Jun 1998. Parameters Z_i denotes the CBL height determined by the gradient method of Sullivan et al. (1998) from rawinsonde observations.

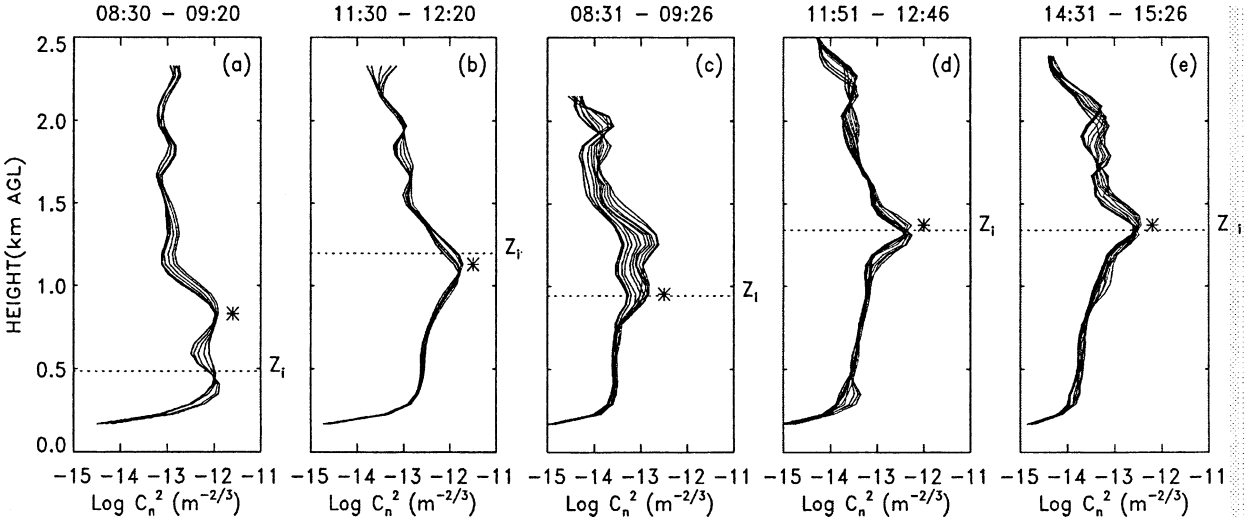

FIG. 4. As in Fig. 3, except for the median filtering method of Angevine et al. (1994). Solid lines represent the C_n^2 profiles of the UHF profiler over the given periods.

range-corrected signal-to-noise ratio (SNR) data observed in cloud-free boundary layers. Angevine et al. (1994) determined a representative CBL height from the median value of the heights at which SNR peaks occurred during a certain period. However, these methods based on maximum backscattered intensity are only applicable for estimating CBL height in cloud-free boundary layers. Dye et al. (1995) used a median profile algorithm to discard the C_n^2 maximum occurring inside scattered fair weather cloud, and pointed out that the estimation of CBL height using their algorithm was nearly inefficient in the case where persistent convective clouds existed above the profiler.

Actually, although UHF radar is a more recent tool used in the boundary layer studies and monitoring, remote sensing of the boundary layer and in particular the determination of Z_i have a long history. The work reported by Kaimal et al. (1982) is a representative example showing CBL depth estimation with a K-band, X-band, and S-band radar, a lidar, and a sodar during the PHOENIX experiment. The remotely determined Z_i level, based on reflectivity profiles, agreed with the CBL depth deduced from different in situ sensors within about $\pm 10\%$. In an earlier study, Campistron (1975) showed the capability of a millimetric radar for the detection of the CBL top and other stable layers located in the free atmosphere.

In the present paper, the behavior of C_n^2 peaks, which is often used to estimate CBL height, is examined, and a new method is suggested that can be used to improve the CBL height estimate from UHF wind profiler observations by making joint use of C_n^2 peaks and vertical air velocity variance σ_w^2. The capability of the present method to estimate the CBL height is analyzed comparing the results obtained by other methods for each of the two cases, a clear day and a cloudy day.

2. Overview of the TRAC experiment: Data collection and processing

a. TRAC experiment

The data used in the present study were collected during the Turbulence, Radar, Aircraft, Cells (TRAC) experiment, the description of which is detailed by Campistron et al. (1999). The experiment was designed to investigate coherent structures in the boudary layer, and to quantify turbulent and coherent transport, surface heat flux and entrainment, and interactions between the boundary layer and clouds. An important goal of the experiment was to provide a relevant database for numerical simulation of the boundary layer. It was carried out from 15 June to 5 July 1998 over a rural flat area of about 60 km $\times$ 60 km located in the middle part of France, several hundred kilometes away from the influence of high mountain ranges and maritime zones. Important instrumental facilities were deployed to reach the scientific objectives. Among them, a C-band Doppler radar, two UHF wind profilers, two powerful sodars, two instrumented aircrafts, and five surface meteorological stations equipped to measure turbulent heat fluxes and other more conventional atmospheric parameters including radiative fluxes were used. Rawinsondes were launched five times a day (0200, 0500, 0800, 1100, and 1400 LST) from the main site of the experiment (48.21°N, 1.68°E) with a typical vertical resolution of about 30 m.

b. UHF profiler

The UHF wind profiler used is the DEGREWIND PCL1300 profiler, designed and manufactured by the Etablissement Degreane. Located at the rawinsonding site, it was operated continuously during the entire cam-

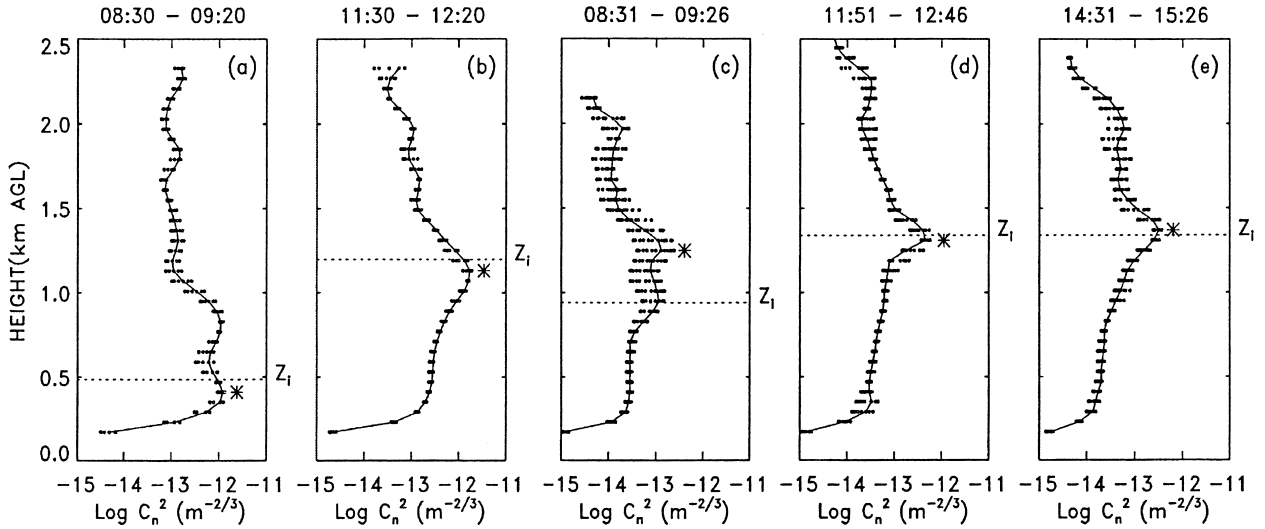

FIG. 5. As in Fig. 3, except for the median filtering method of Dye et al. (1995). Circles indicate the C_n^2 intensity of the UHF profiler at each gate over an hour. Solid lines indicate profiles of the C_n^2 median value taken at each gate.

paign in order to observe mean and turbulent clear air conditions in the lower atmospheric layer. The main characteristics of this Doppler radar were a 1238-MHz transmitted frequency, with a 4-kW peak pulse power, a 25-kHz pulse repetition frequency, and a 150-m pulse length. In order to get the three components of the wind, the profiler alternatively used five beam positions—one vertical and four oblique—with a one-way half-power aperture of 8.5°. The oblique beams, with an off-zenith angle of 17°, were disposed every 90° in azimuth. Signals of time series were acquired with range gates evenly spaced along the radial at 75-m intervals, starting at 65 m AGL. A running coherent integration over 125 points on the times series was performed. In addition, 20 successive Doppler spectra, which were obtained from a 128-point discrete Fourier transform applied on the decimated series (1 point out of 125 points was used), weighted with an Hanning window, were incoherently averaged. As a result, the dwell time on each beam was 13 s, the spectral resolution 0.1 m s^{-1}, and the Nyquist velocity ± 6.1 m s^{-1}.

The spectra, usually contaminated by noise and nonmeteorological echoes, were carefully edited in order to extract the first three moments of the atmospheric backscattered peak. In the first step, the mean noise level was determined using the objective technique proposed by Hildebrand and Sekhon (1974). The zero velocity and the two adjacent spectral lines, usually contami-

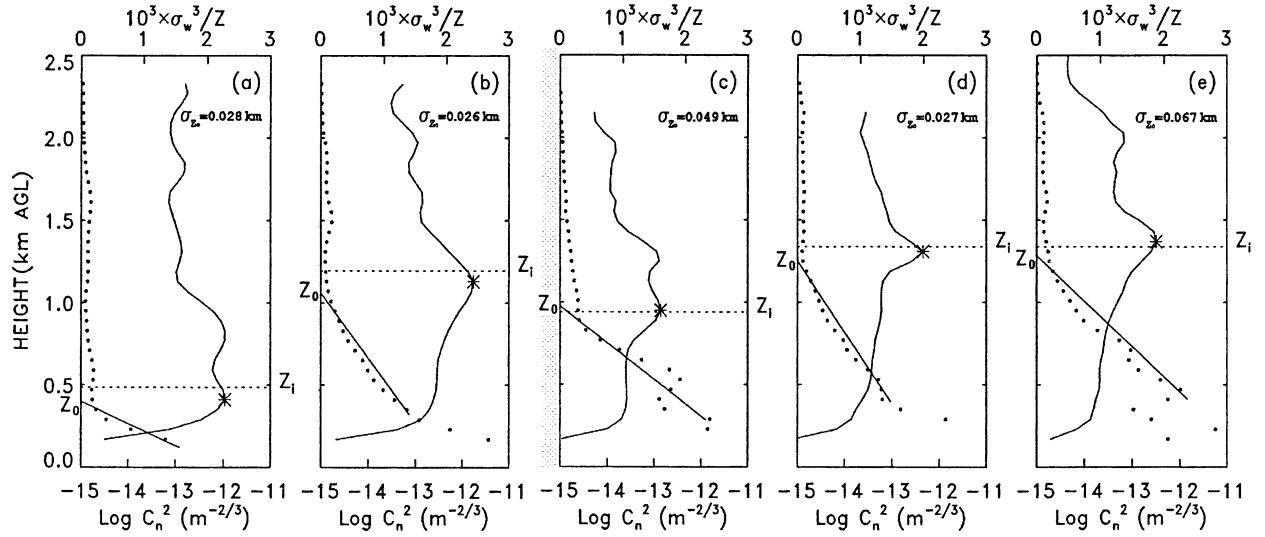

FIG. 6. As in Fig. 3, except for the new method using C_n^2 (solid profile) and σ_w (dotted profile) data. The straight solid lines and Z_0 represent lines of linear regression of the heat flux from the vertical air velocity variance against the height and zero heat flux height estimated by extrapolation of the linear line, respectively. The values for σ_{z0} indicate the uncertainties on the Z_0 intercepts.

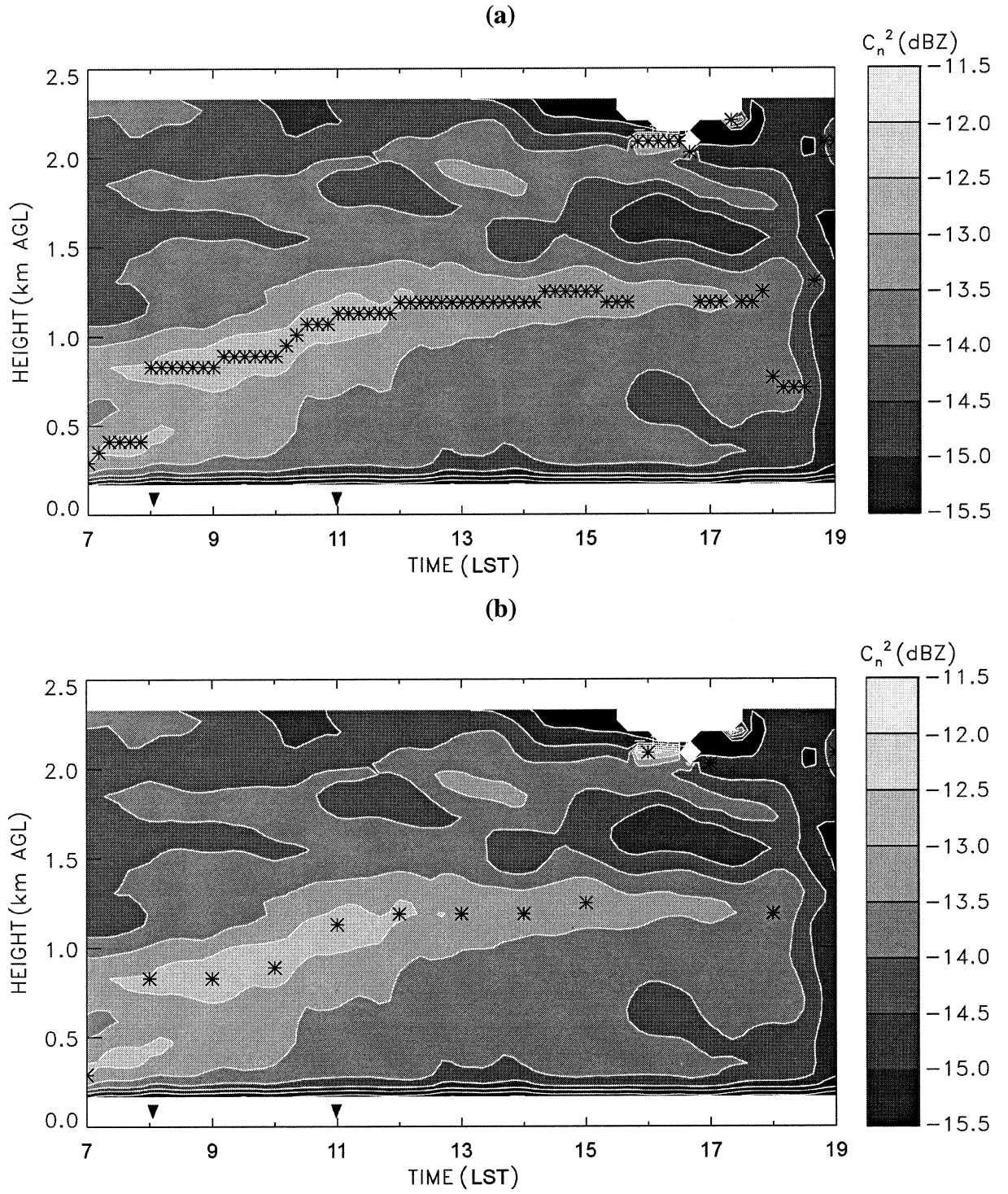

FIG. 7. Time–height cross section of the refractive index structure parameter C_n^2 and CBL heights (asterisks) estimated by (a) the maximum backscatter intensity method (b) the median filtering methods of Angevine et al. (1994) and (c) Dye et al. (1995), and (d) the new method using C_n^2 and σ_w for 19 Jun 1998 at Viabon. Triangles indicate the launch of time soundings during the day.

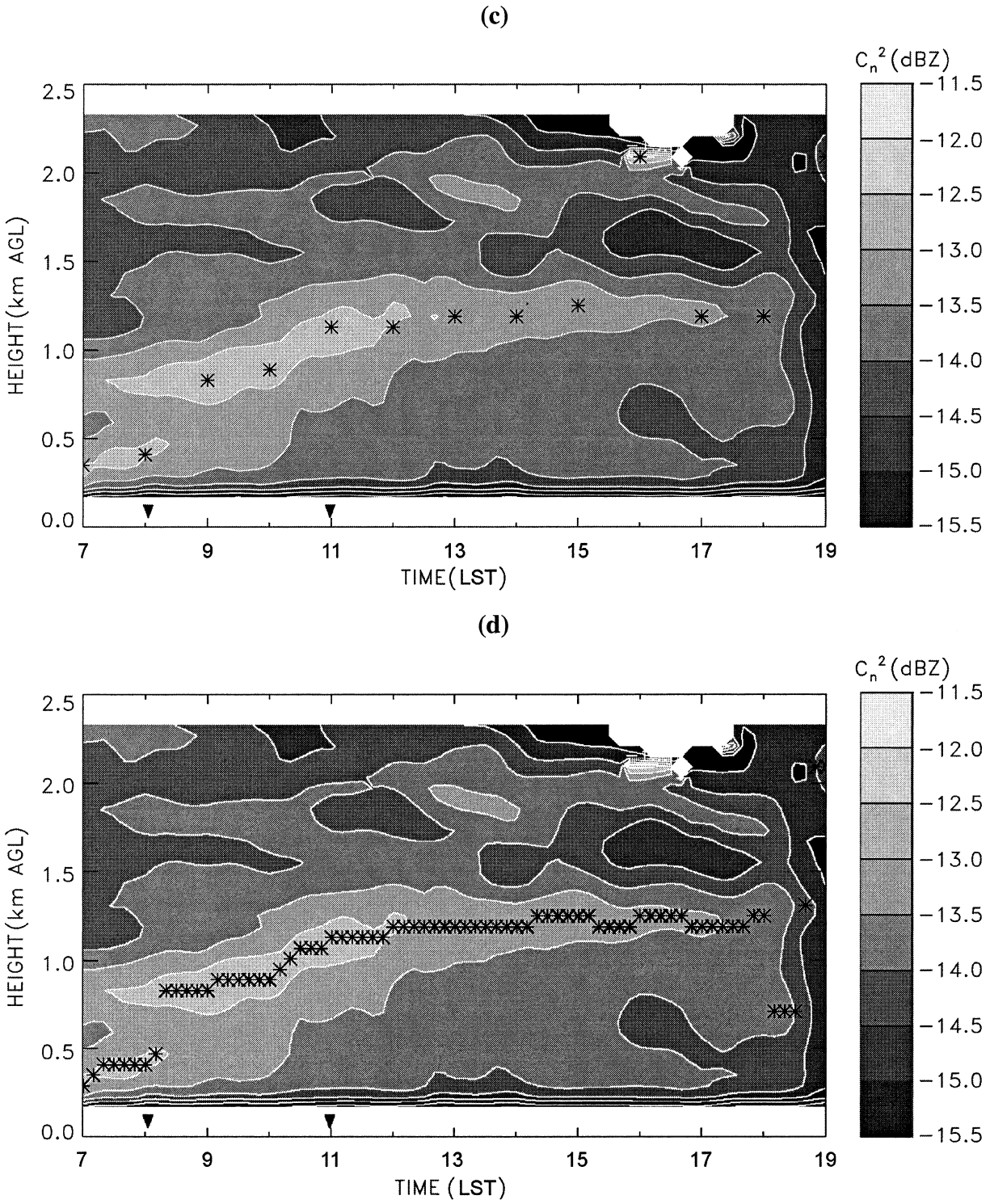

Fig. 7. (*Continued*)

nated by ground clutter, were discarded and replaced by interpolated values. In addition, the statistical averaging technique developed by Merritt (1995) was applied to remove strong coherent-like echoes (bird, aircraft, etc.). Usually, distinct Doppler peaks emerge above the noise level. Thus, in the second step of data processing, the selection of the meteorological peak is done through a consensus based on vertical, temporal, and spectral con-

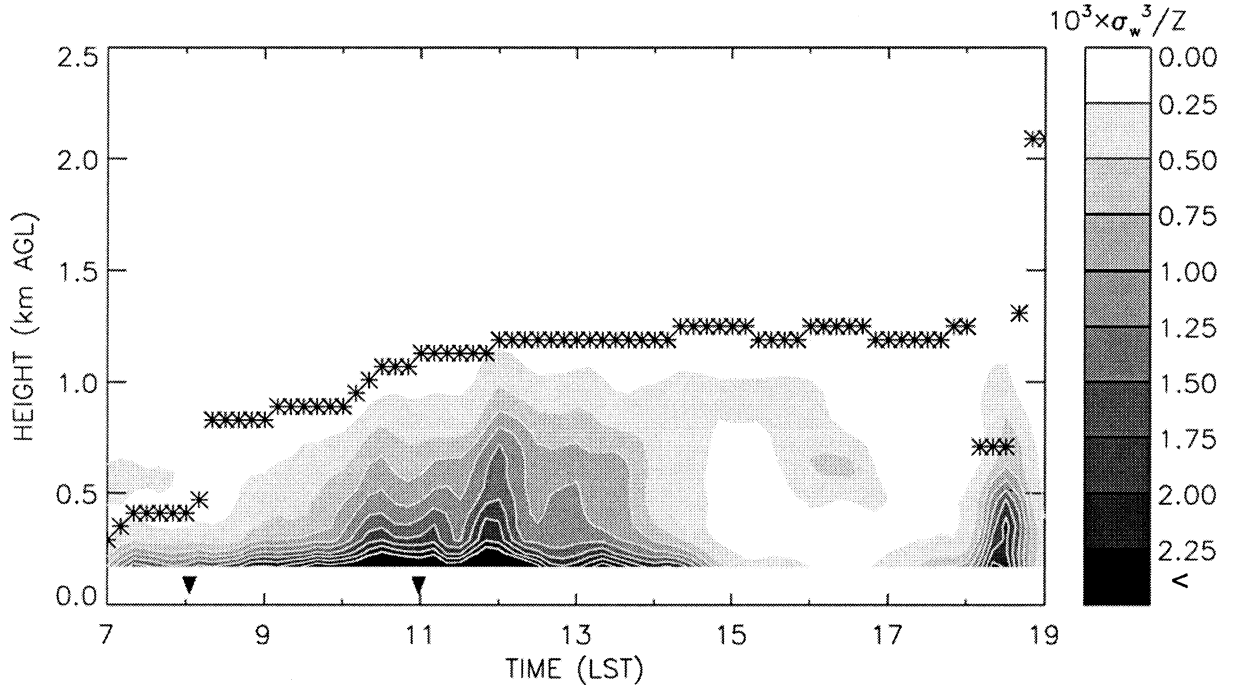

FIG. 8. Time–height cross section of σ_w^3/z with the CBL heights (asterisks) estimated by the new method using C_n^2 and σ_w for 19 Jun 1998 at Viabon.

tinuity as well as thresholding. In fact, the consensus gives a Gaussian weight to each spectral line remaining after thresholding, the value of which depends on the continuity tests. The first three moments are computed with the weighted contiguous spectral lines selected during the last 30 min. Tests have shown that this consensus technique, when removing or smoothing out spurious echoes, performs a temporal average over the considered period of the three moments of the meteorological peak. The use of a consensus period of 5 min or less results in more fluctuating values and sometimes fails to remove unwanted spectral lines. However, when averaging in time, these high-temporal definition moments, the values obtained with the 30-min consensus are recovered. This in particular shows that the spectral width discussed in this paper is not subject to a perceptible broadening factor due to the use of a long-duration-based consensus. Since all the raw Doppler spectra are recorded, it is then possible during offline processing to optimize the parameterization of the consensus to obtain the best results. For the data presented here, we used only a five-beam cycle acquired every 5 min. Additionally, we used only the reflectivity provided by the vertical beam. Tests have shown that reflectivity values acquired on the vertical or oblique beam are in fairly good agreement (with a difference less than 2 dB).

Quality control of the UHF profiler data was made during a 1-yr validation campaign with the use of rawinsondings, sodar, and sonic anemometers (Dessens et al. 1997). On the other hand, the ability of UHF radar to detect rain of even weak intensity was used, in comparison with disdrometer measurements at the ground, to calibrate the instrument in reflectivity and to assess vertical velocity and spectral width retrieval (Campistron et al. 1997).

c. C_n^2 relation

In a turbulent field with a locally homogeneous and isotropic inertial subrange, radar reflectivity due to backscattering from refractive index inhomogeneities is directly proportional to the refractivity structure constant C_n^2 (Tatarskii 1961; Ottersten 1969b). According to Tatarskii (1971), C_n^2 is related to the turbulent field characteristics and to the vertical variation of thermodynamic quantities of the mean field through the following relationship given by Doviak and Zrnic (1993, p. 466):

$$C_n^2 = a^2 \varepsilon^{-1/3} K_\phi 10^{-12} M^2, \tag{1}$$

where a^2 is a dimensionless constant ranging from 3.2 to 4.0, ε is the dissipation rate of turbulent kinetic energy, K_ϕ is the eddy diffusion coefficient of the potential refractivity index, and M is the mean vertical gradient of the generalized potential refractive index. All the quantities in (1) are in Systeme International (SI) units.

Following Ottersten (1969a), M can be formulated as follows:

$$M = -77.6 \times 10^{-6}\frac{P}{T}\left(\frac{d\ \ln\theta}{dz} + \frac{15\ 600q}{T}\frac{d\ \ln\theta}{dz} - \frac{7800}{T}\frac{dq}{dz}\right), \quad (2)$$

where P, T, q, θ, and z are the atmospheric pressure (hPa), temperature (K), mixing ratio (kg kg^{-1}), potential temperature (K), and height (m), respectively.

The CBL top is usually characterized by a strong increase in the potential temperature as well as a strong decrease in the mixing ratio. Thus, these two factors that add positively in (2) enhance the radar signal provided, according to (1), that sufficient turbulent mixing exists to create refractivity index irregularities at half the radar wavelength. This is the principal scale of the inertial subrange participating in the radar signal (Tatarskii 1961).

In a well-mixed CBL, the vertical profiles of potential temperature and mixing ratio are, on average, nearly constant with height (Stull 1988). Despite the strong turbulence, we might expect weak radar echoes from refractive index irregularities in the CBL. Grimsdell and Angevine (1998) have suggested that, in clear-air mixed layers, part of the radar return might be contaminated by hard targets such as insects.

d. Doppler spectra width

In the present work, we make use of the variance of the Doppler spectra σ_w^2 acquired on the vertical beam. According to Sloss and Atlas (1968), σ_w^2 has two principal atmospheric contributors. They are the turbulent velocity fluctuations at scales smaller than the dimension of the radar resolution volume and a broadening factor due to the finite width of the beam. These two contributions are independent of each other and their variances are additive in σ_w^2. The value of the variance σ_b^2 induced by the beam-broadening effect is given by these authors by the following relationship:

$$\sigma_b^2 = \theta_b^2(16\ \ln 2)^{-1}V^2, \quad (3)$$

where V is the horizontal wind speed and θ_b is the one-way half-power angular aperture of the beam assumed to have a Gaussian shape. In the following, we use σ_w^2 values corrected for the beam-broadening effect in order to retain only the turbulent information.

3. Comparison between CBL height estimated from rawinsonde data and UHF C_n^2 profiles

In this section a comparison is made for two characteristic days of TRAC between the vertical profiles of C_n^2 provided by the UHF profiler and the vertical profiles obtained with the rawinsondings of thermodynamical parameters related to C_n^2 in Eq. (2).

a. Definition of the CBL top

As discussed previously in this paper, we consider the CBL top as the height corresponding to the thermal inversion layer (maximum thermal gradient). This definition is totally compatible with both dry and cloudy CBLs where the cloud layer is related to the surface layer, as generally observed in continental conditions. In that case, the CBL height Z_i was determined from rawinsonde data using the gradient method of Sullivan et al. (1998).

b. Analysis of two case studies

For this study, we selected a clear-air CBL (19 June 1998) and a cloud-topped CBL (29 June 1998). They are representative of the main difficulties encountered in Z_i determination using radar. For these two days, the vertical profiles of θ_v, q, virtual potential temperature gradient ($d\theta_v/dz$), and M^2 deduced from rawinsonde observations in the early morning, near midday, and in the midafternoon (only for the cloudy day), are presented in Figs. 1 and 2, respectively. The vertical derivatives were computed using a centered difference at each radiosonde level. A running average over 150 m was applied on the M^2 profiles in order to reduce computing noise. Associated with these thermodynamical parameters, C_n^2 vertical profiles of the UHF profiler obtained shortly around the launch time of the soundings are presented. The rapid decrease of the C_n^2 value, which can be observed below 250 m, is an artifact produced by a range variable attenuation voluntarily introduced to avoid receiver damage from strong returns and transmitter leakage. This artifact does not permit the accurate observation of the CBL properties under a height of 250 m, which corresponds to the early morning state.

1) CASE OF 19 JUNE 1998

On 19 June 1998, the observations were made under fair weather conditions, with a weak synoptic wind of less than 7 m s^{-1} and a nearly cloud free CBL. Figure 1a displays the vertical profiles obtained at about 0800 LST. The profiles of θ_v and its vertical derivative $\partial\theta_v/\partial z$ show two distinct strong stable layers located between 0.3 and 0.7 km and between 1.1 and 1.6 km. These layers are also marked by strong vertical variations of q and correspond to two major peaks in the M^2 profile, a result expected from Eq. (2) considering the vertical evolution of θ_v and q.

The vertical profile of C_n^2 exhibits two distinct peaks with nearly the same magnitude, centered at 0.4 and 0.8 km, respectively. The level of the lower C_n^2 peak coincides with the height of the lower M^2 peak. The other C_n^2 peak is close to a minor peak of the M^2 profile and is in the upper part of a quasi-neutral layer extending from 0.7 to 1 km. This is a typical case in which a C_n^2-based technique might fail in selecting the peak cor-

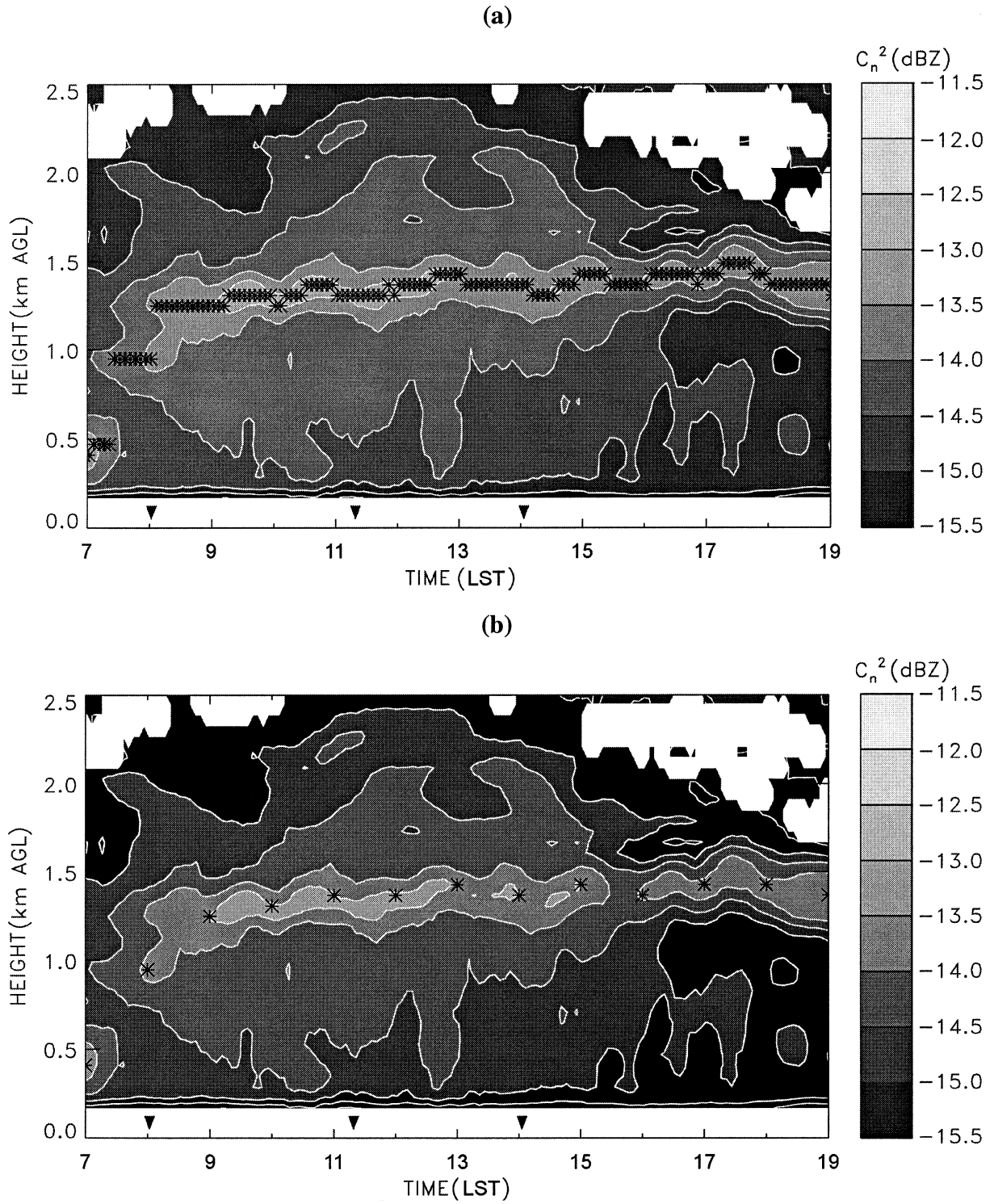

FIG. 9. As in Fig. 7, except for 29 Jun 1998.

responding to the Z_i level unless more information is taken into account.

Considering that these observations were made in the early morning and taking into account the temporal continuity of the UHF observations and rawinsonding measurements, we found that the most probable CBL top is associated with the lower stable layer. Based on the gradient method, the height of the Z_i level was located

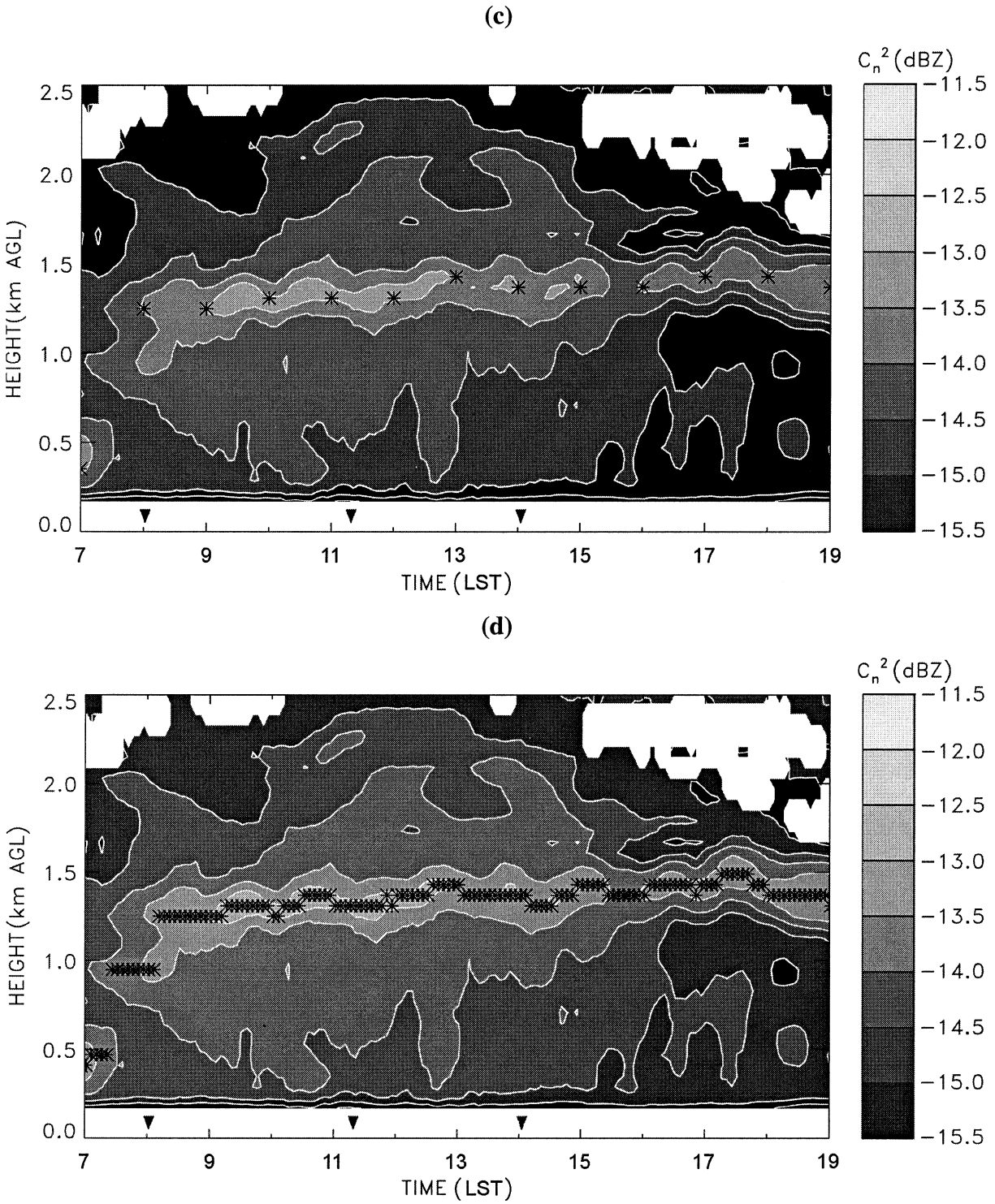

Fig. 9. (*Continued*)

at 0.5 km, that is, 100 m above the corresponding C_n^2 peak. The previously mentioned neutral layer corresponds to the residual layer and the upper-level inversion extending up to 1.6 km might be attributed to the remaining CBL inversion of the previous day or to a synoptic feature. This inversion is not associated with a pronounced wind shear (not shown), which is able to generate dynamic turbulence, and is outside the influence of the turbulent mixing of the CBL. This is an instructive example showing that despite strong tem-

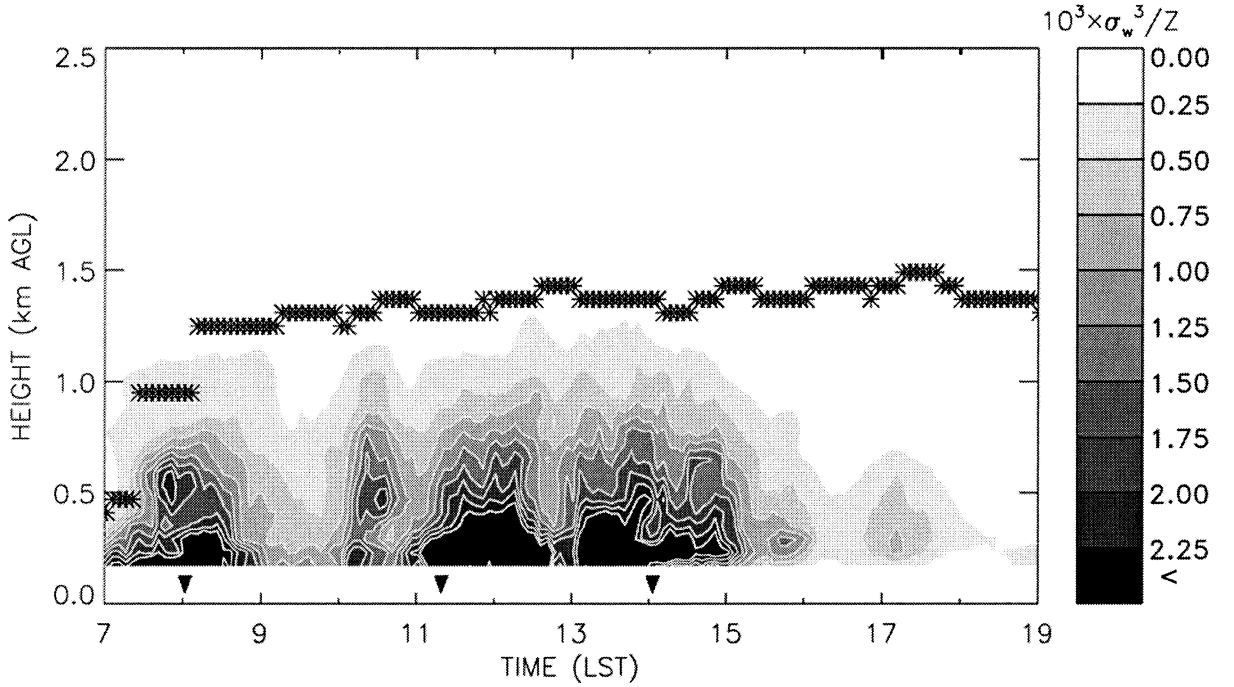

FIG. 10. As in Fig. 8, except for 29 Jun 1998.

perature and humidity gradients but in the absence of sufficient mixing, very slight enhancement in the radar signal occurs.

At about 1100 LST on the same day, the vertical profiles presented in Fig. 1b show that the estimations of the CBL height are simpler than in the early morning. We are left with a C_n^2 profile with a single prominent maximum located at a height of about 1.15 km. This level is about 50 m below the heights of M^2 and $\partial\theta_v/\partial z$ maxima, near the base of a temperature inversion extending from 1.1 to 1.3 km. Beneath this layer, the CBL appears well mixed with nearly constant θ_v and q profiles. The gradient method gives a Z_i level at 1.2 km, in good concordance with the C_n^2 peak.

2) CASE OF 29 JUNE 1998

On 29 June 1998, a humid but weak (less than 6 m s^{-1}) westerly flow prevailed in the CBL. Figures 2a to 2c present vertical profiles obtained from radiosondes and UHF radar at about 0802, 1119, and 1403 LST, respectively. This fair weather day differs from the first case study because of the partly cloudy sky present from early morning to late afternoon with cloud fraction varying from 60% to 80%, according to visual reports made at the UHF site. Radiosonding offers only a snapshot in time and space of the atmosphere. Thus, in order to get a more complete description of the cloud layer, we used measurements collected by one of the two research aircraft that performed continuous flights over the study area between 0916 and 1207 LST.

This flight was divided into eight 45-km constant levels and course legs between 100 and 1800 m above ground and centered on the vertical of the UHF. Four legs were performed in a north–south-oriented vertical plane and the other in an east–west-oriented vertical plane. Following Grimsdell and Angevine (1998), the cloud-base height was taken to be the lifting condensation level deduced from the aircraft data series of pressure, temperature, and mixing ratio sampled along the flight every 4 m. The results for the considered flight period show a mean cloud-base height of 800 m and an increase in the cloud base of about 150 m toward both the north–south and the west–east directions over the 45-km legs. In addition, on average, there was a temporal increase of about 120 m during the 3-h flight. At the beginning of the flight, during the ascent, the aircraft crossed the cumulus layer and visual report indicated a cloud-base and cloud-top height of 900 and 1400 m, respectively. The same observations made at the end of the flight situated the cloud-base and cloud-top level at about 950 and 1400 m, respectively.

The early morning vertical profiles at 0802 LST in Fig. 2a display similar characteristics to those of the previously discussed day (Fig. 1a). With the same reasoning, we identify a residual layer including clouds, between about 1.0 and 1.3 km, with a nearly constant virtual potential temperature with height, capped by a stable layer extending, from 1.3 to 1.45 km. In this inversion layer, the vertical increase of the potential temperature and the vertical decrease of the mixing ratio are much more acute than in the case of the cloud-free day. The most probable CBL top in Fig. 2a is found at about 0.9 km, at the base of a weakly stable layer where

some thin clouds could be identified. This level corresponds to the height of one of the two main peaks, with nearly the same intensity, of the radar–C_n^2 profile. The second C_n^2 peak at a height of 1.3 km is linked to the base of the strong inversion aloft but is displaced 150 m below the well-defined M^2 peak positioned in the upper part of this stable layer. There is a third distinct but less prominent peak C_n^2 near a height of 1.9 km, located at the base of an increase of the virtual potential temperature and at the same level of the M^2 maximum, which can be linked with the cloud layer disconnected from the CBL.

Around midday (Fig. 2b) and midafternoon (Fig. 2c) only one prominent C_n^2 peak existed at about 1.4 km, coincident with a M^2 maximum at the base of a strong inversion layer. Without ambiguity, this level can be defined as the CBL top in view of the well-mixed potential temperature and mixing ratio profiles beneath. Secondary relatively weak peaks of C_n^2 are apparent at a height of 2.3 km (Fig. 2b) and at 2.0 km (Fig. 2c), and are not correlated with an evident singularity in the radiosonde profiles. However, at a height of 1.4 km, the C_n^2 peak in Fig. 2c was produced by mixing at the cloud top.

3) CONCLUDING REMARKS

In summary, the analysis of these two case studies shows ambiguity in the determination of the Z_i from C_n^2 peaks, mainly in the early development of the CBL when a residual layer from the previous day persists. In the presence of clouds, the C_n^2 peak is always very close to the CBL depth defined at the level of the capping inversion layer. However, due to the cloud-base variability deduced from aircraft measurement, it is not possible to conclude that the cloud base was also positioned at the CBL top. However, the cloud top seems to be associated with a secondary radar reflectivity maximum. Finally, distinct peaks of the mean vertical gradient of the generalized potential refractive index are apparently not always linked to the local maximum of observed C_n^2. As expected from Eq. (1), to understand radar return intensity it is necessary to take into account the degree of small-scale turbulent mixing.

4. Estimation of the CBL height with C_n^2-based techniques

Two main algorithms to estimate the CBL height from UHF profiler data have been suggested by several researchers, as quoted in the introductory section. These algorithms are based on the entrainment-induced maximum of backscatter intensity, such as maximum value of SNR or C_n^2, and are compared and tested by estimating the CBL height for two cases—a clear day and a cloudy day.

a. Maximum backscattered intensity method

This method, proposed by White (1993), simply assigns the CBL height as the level of C_n^2 or SNR maximum in an instantaneous vertical profile. Figure 3 shows vertical profiles of UHF backscatter intensity and the CBL heights estimated by the maximum backscattered intensity method at 0800 and 1100 LST on 19 June 1998, and at 0801, 1121, and 1401 LST on 29 June 1998. Except for Fig. 3a, the CBL heights deduced from the C_n^2 peaks agreed with the rawinsonde-estimated CBL heights. In the case of Fig. 3a, the C_n^2 profile had a double peak structure where the primary and secondary peaks occurred from the residual layer and the CBL height, respectively.

The maximum backscattered intensity method takes the primary C_n^2 peak as the CBL height. This method, therefore, has a tendency to erroneously estimate a C_n^2 peak due to the enhancement of reflectivity by a cloud layer or a stable residual layer when the C_n^2 profile had a double peak structure as in Fig. 3a. However, the method can provide a good time resolution in the estimation of CBL height since it estimates the height from the C_n^2 maximum of a single profile.

b. Median filtering method

This method is based on an increase in backscatter intensity in the same way as the maximum backscattered intensity method. However, a median filter is used to remove C_n^2 peaks from the enhancement of reflectivity by clouds, stable residual layer, precipitation, and biological targets such as insects and birds.

Angevine et al. (1994) suggested two algorithms to find CBL height. In the first, a C_n^2 peak in each profile is selected and then the median value of the heights at which the peaks occur during the considered period is determined to be the CBL height. The other is that after taking the median value of the C_n^2 values at each range gate during the considered period, the height that has the peak value in the median C_n^2 profile is determined as the CBL height. Dye et al. (1995) included threshold logic to remove the enhancement of reflectivity by nonmeteorological targets such as migrating birds, aircraft, and so on and computed the median C_n^2 value at each range gate over a period. They then selected the height of the maximum C_n^2 in the median profile as the CBL height for that period. The threshold removes all values of C_n^2 greater than 10^{-11} m$^{-2/3}$.

Vertical profiles of UHF backscattered intensity and the CBL heights determined from the first median filtering method of Angevine et al. (1994) are shown in Fig. 4. The solid lines in each panel represent the C_n^2 profiles during the observation. Except for Fig. 4a, the CBL heights estimated using this method agreed with the rawinsonde-estimated CBL heights. In the case of Fig. 4a, the heights of the primary peaks from the residual layer were constant, while the heights of the sec-

ond peaks from the CBL height were raised with a lapse in time. This method, therefore, erroneously estimated the height at which the primary peaks consistently occurred as the CBL height.

Vertical profiles of UHF-backscattered intensity and the CBL heights determined from the median filtering method of Dye et al. (1995) for the same case as Figs. 3 and 4 are shown in Fig. 5. In the case of Fig. 5a, with both elevated residual layer and CBL height, this method determined the lower C_n^2 peak as the CBL height. However, in the case of Fig. 5c, where cloud layers were distinct from the CBL height, the upper C_n^2 peak due to cloud layer was selected as the CBL height during the considered period. According to these results, this method has a tendency to estimate heights at which the C_n^2 values and their fluctuations with time were as large as the CBL height. In the case of a rapidly growing CBL in the morning or a very fluctuating cloud top, this method may produce inaccurate estimates of CBL height.

The median filtering methods of Angevine et al. (1994) and Dye et al. (1995) performed best when scattered fair weather cumulus clouds were present or vertical profiles of backscatter intensity had a single peak structure, but performed worst when deep clouds were persistently present over the UHF radar or vertical profiles of backscattered intensity had a double peak structure. These algorithms find a representative CBL height from several profiles of backscattered intensity observed during an hour. Consequently, these methods provide CBL height estimations of lower time resolution than the maximum backscattered intensity method, which can estimate its height from a single profile (in about 10 min).

5. Estimation of CBL height using C_n^2 and σ_w^2 profiles

The fourth method introduced here is a proposed improvement to the existing methods by making use of the UHF Doppler spectral width. The maximum backscattered intensity method and median filtering method were found to be incomplete in their estimations of CBL height when the backscattered intensity profile had a double peak, and the primary peak in each profile occurred in cloud layers or at the top of a residual layer rather than at the top of the mixed layer. In this paper, an algorithm is proposed to distinguish the peak caused by CBL height from other peaks due to either a cloud layer or a residual layer. This is done by using the variance of vertical air velocity measured by a UHF profiler.

In a dry, convectively well-mixed layer, heat flux decreases linearly with height from the ground to the top of CBL, where it reaches a minimum. The heat flux profile is linked with the standard deviation of the vertical velocity by the relation (Weill et al. 1980)

$$\frac{\sigma_w^3}{z} \approx \alpha^{3/2}\frac{g}{\theta}(\overline{w'\theta_v'}), \tag{4}$$

where σ_w, z, and α represent the standard deviation of the turbulent vertical velocity, height, and a universal constant ($\alpha = 1.4$), respectively. The term (g/θ) $(\overline{w'\theta_v'})$ represents a local buoyancy production, where g, θ, θ_v, and w' are the gravitational acceleration, potential temperature, virtual potential temperature, and vertical velocity perturbation, respectively. Implicitly, this relation implies that the profile of vertical velocity standard deviation is linked with the CBL sensible heat flux profile. In a well-mixed layer, the heat flux decreases linearly with height. Consequently, σ_w^3/z in Eq. (4) decreases linearly from the top of the surface layer to the CBL top. To find CBL height, the present method employs a comparison of the C_n^2 peak heights with the height corresponding to the ''zero flux level'' (the level where σ_w^3/z becomes null), which is deduced from the vertical profile of the variance of the vertical velocity (see Fig. 6). The nearest peak of C_n^2 peaks to the zero flux level is taken as the CBL height. This level implies that there is a continuity of turbulent motion between the ground and the selected level. In cloudy conditions, this condition is only correct within the mixed layer up to the cloud base.

The new method follows three steps to find the reference height using the σ_w^3/z profile, and then to determine the CBL height from the C_n^2 peaks.

First, the primary and secondary peaks were selected in each C_n^2 profile, and the height of a peak close to the surface was chosen as our first guess of the CBL height Z_1. The selection of the lowest peak ensures that the data below it are inside the mixed layer.

Second, a linear regression line of Eq. (4) was obtained by least square fitting between the preceding estimation of Z_1 and $0.2Z_1$. The lower bound ($0.2Z_1$) secures the only data in the mixed layer for the least square fitting. Therefore, the values of σ_w^3/z in the surface layer are not used in the least square fitting. This restriction is required because the relation (4) is correct only in the mixed layer and the UHF profiler data may not be satisfactory below 200 m.

Third, the zero heat flux height, Z_0 was estimated by an extrapolation of the regression line as shown in Fig. 6. Therefore, the height of the C_n^2 peak nearest to Z_0 was taken as the CBL height.

Figure 6 shows the vertical profiles of UHF-backscattered intensity and CBL height determined using C_n^2 and σ_w data of UHF profilers for the same case as in Fig. 4. The height of the zero heat flux in Fig. 6 was found to be near the radiosonde-estimated CBL heights; the new method estimated the CBL heights well even though the profile had double peaks. The uncertainties in the Z_0 intercepts in Figs. 6a–e are 0.028, 0.026, 0.049, 0.027, and 0.067 km, respectively, and the distances between the two C_n^2 peaks in Figs. 6a and 6c are 0.420 km and 0.300 km, respectively. As in the cases of Figs.

6a and 6c, the errors of the zero intercepts are much smaller than the distances between the two peaks. Thus, the peak closest to the intercept is well identified as the CBL height.

6. Estimation of diurnal variation of CBL height

Four methods, as previously mentioned, were compared and analyzed to examine their ability to estimate the diurnal variation of CBL height during a clear day and a cloudy day. In addition, the time resolution of the analyzed CBL heights was compared using the diurnal variations of the CBL heights obtained by the four different methods.

The CBL heights were estimated from the vertical profiles of UHF backscattered intensity on a clear day using four different methods. The diurnal variations of CBL height are shown in Fig. 7 for 19 June 1998. According to the strongest peak in the time–height cross section of C_n^2, around 0700 LST, the CBL formed and started growing. Its height grew rapidly from 0.3 km at 0700 LST to 1.1 km at 1100 LST and reached nearly 1.3 km around 1200 LST. It ranged between approximately 1.2 and 1.3 km during the afternoon. After 1700 LST, corresponding to sunset, the 1.3-km inversion level corresponded to the top of the residual layer. A stable layer was formed near the ground that grew throughout the night. Our comments on the mixed layer are correct only up to 1700 LST, where the surface heat fluxes are always in relation to the CBL top.

The diurnal variations of CBL heights derived from the maximum backscattered intensity method shown in Fig. 7a agree well with the rawinsonde-estimated CBL heights and also provided reasonable structure and evolution of the CBL during the growth of the CBL height. During the late afternoon between 1600 and 1750 LST, however, this method overestimated the CBL height when partial clouds were persistently present at 2.1 km and higher. Figures 7b and 7c show the diurnal variations of the CBL heights determined by the median filtering method of Angevine et al. (1994) and Dye et al. (1995), respectively. The results are similar to that of the CBL heights estimated by the maximum backscattered intensity method. The diurnal variations of the CBL heights estimated by the new method using C_n^2 and σ_w data are shown in Fig. 7d. The results of the CBL height derived from the new method agree well with not only the rawinsonde-estimated CBL heights but also provide also a reasonable structure and evolution of the CBL height without overestimation in the presence of partly persistent clouds. This method also gives a good time resolution for CBL height detection. Figure 8 clearly shows that the parameter σ_w^3/z is at its maximum during daytime near ground level and decreases from the ground to the top of the boundary layer in relation to the turbulence inside the CBL. The maximum of σ_w^3/z is well linked with the maximum of radiative energy, which arrives at ground level. During the period between 1800 and 1900 LST, the singularities of σ_w^3/z was observed by the UHF profiler.

The diurnal variations of the CBL heights on a cloudy day estimated by four different methods are shown in Fig. 9. Considering both the variation of the strongest peak in the time–height plots of C_n^2 and the rawinsonde-estimated CBL heights, the CBL height grew rapidly from 0.5 km at 0700 LST to 1.2 km at 0830 LST. Additionally, the elevated CBL height coincided with the top of the cloud layer. After 0830 LST, it was controlled by the cloud layer and fluctuated between approximately 1.2 and 1.4 km. Sharp variations in both θ_v and q at the top of the CBL and significant turbulence within the cloud layers resulted in the reflectivity enhancement between 1.2 and 1.4 km and a narrow width of the C_n^2 contour of more than -12.5 dB. The sharp peaks due to reflectivity enhancement aided the estimation of the CBL height in all four method, and allowed the attainment of a reasonable structure and evolution of the CBL except for the case in which the median filtering method of Dye et al. (1995) overestimated the CBL height around 0800 LST. In this case, the new method estimated the CBL heights well and provided a reasonable structure and evolution of the CBL without overestimation in the presence of partly persistent clouds. Figure 10 shows, as in Fig. 8, that the parameter σ_w^3/z represents the evolution of the turbulence inside the CBL between 0700 and 1700 LST. During this day, the turbulence evolution is very different from the previous case with a clear sky and seems to be modulated by the cloud cover. As in the previous case, this parameter clearly shows that the turbulent structure is well linked with the CBL top deduced from C_n^2.

7. Summary and conclusions

In the present study, the applicability of C_n^2 peaks in the estimation of CBL height was investigated and a new method to objectively estimate the CBL height using C_n^2 and σ_w data of UHF profilers was developed. This method was compared with other methods for two cases, one on a clear day and the other on a cloudy day.

The peaks in each C_n^2 profile often occurred not only at the top of the CBL but also at the residual layer. When there was no significant solar heating and vertical mixing in the morning, the height of the strongest vertical gradient of θ_v was not consistent with that of a strong vertical gradient of q. When the vertical gradients of θ_v and q in the entrainment zone were very strong due to strong vertical mixing in the afternoon, the C_n^2 peak corresponding to the CBL height was in good agreement with the rawinsonde-estimated CBL height. If there were cloud layers or a residual layer over the top of the CBL height, the vertical profile of backscattered intensity had a double peak structure. In particular, when the CBL height was consistent with the height of the cloud layer, vertical profiles of both $d\theta_v/dz$ and C_n^2 had a sharp peak near the top of the cloud layer

because of the strong vertical gradient of θ_v due to the entrainment mixing near cloud boundaries and at the entrainment zone.

The maximum backscattered intensity method and median filtering method correctly estimated the CBL height when the C_n^2 profile had a single peak, but these methods erroneously estimated the CBL height when there was a residual layer or a cloud layer over the CBL. The new method distinguished the peak due to the CBL height from the peak due to a cloud layer or a residual layer by using both C_n^2 and σ_w data. It was then able to correctly estimate the CBL height. With regard to diurnal variations of the CBL height, the new method provided more stable and reliable estimations of CBL heights in real time than the other methods even when the vertical profiles of backscattered intensity had two peaks around CBL height due to a residual layer or cloud layer.

The new method developed in this study can estimate CBL height using C_n^2 and σ_w data as well as provide information about the evolution of CBL height over the entire day. The analysis was based on two case studies and more observations are indeed needed to confirm the reliability of the proposed method of Z_i determination.

Acknowledgments. The TRAC experiment was mainly funded by the Institut National des Sciences de l'Univers (INSU), Météo-France and Electricité De France (EDF). Two authors (Kim and Heo) gratefully appreciate the financial support of the Korea Science and Engineering Foundation Grant KOSEF 985-0400-004-2.

REFERENCES

Angevine, W. M., A. B. White, and S. K. Avery, 1994: Boundary layer depth and entrainment zone characterization with a boundary-layer profiler. *Bound.-Layer Meteor.,* **68,** 375–385.

Benech, B., B. Campistron, J. Dessens, S. Jacoby-Koaly, E. Dupont, and B. Carissimo, 1997: Comparison of turbulence measurements in the atmospheric boundary layer by UHF profiler, sodar and sonic anemometer. *Proc. Eighth Int. Workshop on Technical and Scientific Aspects of MST Radar,* Bangalore, India, Solar-Terrestrial Energy Program, 111–114.

Beyrich, F., and A. Weill, 1993: Some aspects of determining the stable boundary layer depth from Sodar data. *Bound.-Layer Meteor.,* **63,** 97–116.

Burk, S. D., 1980: Refractive index structure parameters: Time-dependent calculations using a numerical boundary layer model. *J. Appl. Meteor.,* **19,** 562–576.

Campistron, B., 1975: Characteristic distributions of angel echoes in the lower atmosphere and their meteorological implications. *Bound.-Layer Meteor.,* **9,** 411–426.

——, B. Bénech, J. Dessens, S. Jacoby-Koaly, E. Dupont, and B. Carissimo, 1997: Performance evaluation of a UHF boundary layer radar in raining conditions based on disdrometer measurements. *Proc. Eighth Int. Workshop on Technical and Scientific Aspects of MST Radar,* Bangalore, India, Solar-Terrestrial Energy Program, 334–337.

——, and Coauthors, 1999: The turbulence radar aircraft cells. Preprints, *13th Conf. on Boundary Layers and Turbulence,* Dallas, TX, Amer. Meteor. Soc., 620–623.

Deardorff, J. W., G. E. Willis, and B. H. Stockton, 1980: Laboratory studies of the entrainment zone of a convectively mixed layer. *J. Fluid Mech.,* **100,** 41–64.

Dessens, J., B. Bénech, B. Campistron, S. Jacoby-Koaly, E. Dupont, and B. Carissimo, 1997: A one year UHF validation campaign using rawinsondings, sodar, anemometers and disdrometer. Proc. *Eighth Int. Workshop on Technical and Scientific Aspects of MST Radar,* Bangalore, India, Solar-Terrestrial Energy Program, 200–203.

Doviak, R. J., and D. S. Zrnic, 1993: *Doppler Radar and Weather Observations.* Academic Press, 562 pp.

Dye, T. S., C. G. Lindsay, and J. A. Anderson, 1995: Estimates of mixing depth from boundary layer radar profilers. Preprints, *Ninth Symp. on Meteorological Observations and Instrumentation,* Charlotte, NC, Amer. Meteor. Soc., 156–160.

Fairall, C. W., 1991: The humidity and temperature sensitivity of clear air radars in the convective boundary layer. *J. Appl. Meteor.,* **30,** 1064–1074.

Grimsdell, A. W., and W. M. Angevine, 1998: Convective boundary layer height measurement with wind profilers and comparison to cloud base. *J. Atmos. Oceanic Technol.,* **15,** 1331–1338.

Hildebrand, P. H., and R. S. Sekhon, 1974: Objective determination of noise level in Doppler spectra. *J. Appl. Meteor.,* **13,** 808–811.

Kaimal, J. C., N. L. Abshire, R. B. Chadwick, M. T. Decker, W. H. Hooke, R. A. Kropfli, W. D. Neff, and F. Pasqualucci, 1982: Estimating the depth of the daytime convective boundary layer. *J. Appl. Meteor.,* **21,** 1123–1129.

Merritt, D. A., 1995: A statistical averaging method for wind profiler Doppler spectra. *J. Atmos. Oceanic Technol.,* **12,** 995–1001.

Muschinski, A., P. P. Sullivan, D. B. Wuertz, R. J. Hill, S. A. Cohn, D. H. Lenschow, and R. J. Doviak, 1999: First synthesis of wind-profiler signals on the basis of large-eddy simulation data. *Radio Sci.,* **6,** 1437–1459.

Ottersten, H., 1969a: Mean vertical gradient of potential refractive index in turbulent mixing and radar detection of CAT. *Radio Sci.,* **4,** 1247–1249.

——, 1969b: Radar backscattering from the turbulent clear atmosphere. *Radio Sci.,* **4,** 1251–1255.

Sloss, P. W., and D. Atlas, 1968: Wind shear and reflectivity gradient effects on Doppler radar spectra. *J. Atmos. Sci.,* **25,** 1080–1089.

Stull, R. B., 1988: *An Introduction to Boundary Layer Meteorology.* Kluwer Academic, 666 pp.

Sullivan, P. P., C.-H. Moeng, B. Stevens, D. H. Lenschow, and S. D. Mayor, 1998: Structure of the entrainment zone capping the convective atmospheric boundary layer. *J. Atmos. Sci.,* **55,** 3042–3064.

Tatarskii, V. I., 1961: *Wave Propagation in a Turbulent Medium.* McGraw-Hill, 285 pp.

——, 1971: *The Effects of the Turbulent Atmosphere on Wave Propagation.* U.S. Dept. of Commerce, 472 pp.

Weill, A., C. Klapisz, B. Strauss, F. Baudin, C. Jaupart, P. van Grunderbeck, and J. P. Goutorbe, 1980: Measuring heat flux and structure functions of temperature fluctuations with an acoustic Doppler sodar. *J. Appl. Meteor.,* **19,** 199–205.

White, A. B., 1993: Mixing depth detection using 915-MHz radar reflectivity data. Preprints, *Eighth Symp. on Meteorological Observations and Instrumentation,* Anaheim, CA, Amer. Meteor. Soc., 248–250.

Wyngaard, J. C., and M. A. LeMone, 1980: Behavior of the refractive index structure parameter in the entraining convective boundary layer. *J. Atmos. Sci.,* **37,** 1573–1585.